Ambient-dried thermal superinsulating monolithic silica-based aerogels with short cellulosic fibers

Gediminas Markevicius, Rachid Ladj, Philipp Niemeyer, Tatiana Budtova, Arnaud Rigacci

J. Material Science, **52**, 2210–2221 (2017) DOI: 10.1007/s10853-016-0514-3

Ambient-dried thermal superinsulating monolithic silica-based aerogels with short cellulosic fibers

Gediminas Markevicius[1, 2], Rachid Ladj[1, 2], Philipp Niemeyer[1, 2], Tatiana Budtova[2]*, Arnaud Rigacci[1]*

[1] MINES ParisTech, PSL Research University, PERSEE - Centre for processes, renewable energy and energy systems, CS 10207 rue Claude Daunesse, 06904 Sophia Antipolis Cedex, France

[2] MINES ParisTech, PSL Research University, CEMEF - Centre for Materials Forming, CNRS UMR 7635, rue Claude Daunesse, CS 10207, 06904 Sophia Antipolis Cedex, France

Corresponding authors:

Tatiana Budtova: Tatiana.Budtova@mines-paristech.fr ,+33493957470

Arnaud Rigacci: Arnaud.Rigacci@mines-paristech.fr , +33493957494

Authors' emails:

Gediminas Markevicius: gediminas.markevicius@mines-paristech.fr

Rachid Ladj: rladj@live.fr

Philipp Niemeyer: philipp.niemeyer@dlr.de

Abstract

Short (< 2.5 mm) cellulose fiber–silica composite aerogels were synthesized by dispersing cellulose fibers in polyethoxydisiloxane based sol. After in situ gelation, silica phase was hydrophobised with hexamethyldisilazane, and the composites were dried either at ambient pressure or with supercritical (sc) CO_2. Fiber concentration was varied from 0 to 25 wt% (corresponding to 0 – 2.1 vol %) of the final dried composite. Preformed cellulosic fiber network preserved the monolithic shape of the silica-based composites during ambient drying. At room conditions, thermal conductivities were 0.015 ± 0.001 W/(m.K) for sc dried aerogels and 0.017 ± 0.001 W/(m.K) for their ambient dried counterparts. Materials dried with either method exhibited large specific surface areas, from 570 to 730 m^2/g, and SEM analysis did not show significant differences in the global structure of the silica network. Composite aerogels were hydrophobic with water contact angles around 138 °. Based on this proof of concept, the same approach was used with a variety of natural and recycled cellulosic fibers also resulting in silica-based monoliths with low thermal conductivities in the 0.016-0.023 W/(m.K) range, all produced via ambient drying.

Keywords

Aerogel; silica; cellulose; fiber; composite; ambient-drying; thermal conductivity

Introduction

Silica aerogels exhibit remarkably low thermal conductivities, e.g. as low as 0.013 W/(m.K) in room conditions [1-3], and promise interesting sound abating properties [4] which make them extremely desirable as new type of advanced thin insulation materials [5-7]. This is especially important for the applications where the geometrical constrains regarding to space are of importance, such as insulating older buildings from inside with minimum reduction of living surface, as well as in automotive and aerospace industry. Thermal super-insulating properties (formally, conductivity below that of air in ambient conditions, 0.025 W/(m.K)) of the silica aerogels are primarily due to the Knudsen effect in the porous network [8, 9] combined with their low density, high degree of porosity (> 90%), nanostructured and tortuous solid backbone and rather low radiative contribution in room conditions [10].

Aerogels are typically synthesized via sol-gel process, and solvent is removed via supercritical (sc) drying [11, 12]. The latter is used in order to avoid intense capillary pressure, and in particular pore's liquid/gas surface tension, which induces the collapse of most of the pores during standard evaporative drying. However, supercritical drying remains considered by some industrial players as a major drawback in the upscaling and wide commercialization of the aerogel-based insulation components due to a time consuming process which involves high pressures and various process limitations. Subcritical (or sometimes "ambient") drying therefore is much desired and is actively studied for preparing materials with properties similar to their sc counterparts.

To avoid irreversible pore collapse during ambient pressure drying, grafting of the pore walls with incondensable moieties (for example, silylation) is usually performed [13, 14]. It leads to the "spring-back effect", i.e. re-opening of the pores during the last stage of drying due to the repulsion of the grafted groups and elasticity of the solid network. However, due to

the inherent brittleness of nanostructured silica network, the initial monolithic shape of the gel is not preserved [15, 16]: the resulting material is aerogel-like divided solid (e.g. “granular bed” or powder). To keep the matter monolithic, composite approach is applied. It consists of using nonwoven fibrous mats to maintain macroscopic cohesion of silica after drying. Fibers are usually glass or based on synthetic polymers. Such flexible products – so-called *blankets* - are now produced at industrial level [17, 18]. Similar works have been recently conducted at laboratory scale using organically modified silica precursors like methyltrimethoxysilane (MTMS) which also promotes spring-back effect and confer, at the end, monolithicity and very low thermal conductivity together with hydrophobicity [19].

Other routes, such as strengthening during ageing by dissolution-precipitation mechanisms have been studied in the past [20]. More recently, a lot of work was dedicated to hybrids [21] and composites [22, 23]. Good mechanical strengthening has been obtained while keeping low thermal conductivity values [24, 25]. However, to the best of our knowledge, very few publications report these aerogels obtained with ambient-drying [25, 26].

In this work we demonstrate how short (< 2.5 mm) cellulose fibers can also aid in fabrication of monolithic ambient-dried aerogels while maintaining overall properties of silica aerogel, such as low density, mesoporosity, high specific surface area, and extremely low thermal conductivity. Cellulose fibers are particularly attractive for this application due to their abundance, low cost, and environmental friendliness. Natural fibers have been demonstrated to improve mechanical properties of polymer composites [27, 28]. They are generally viewed as a viable and environmentally friendly replacement of glass fibers [29], which are currently widely used in composite and insulation materials. Till now, nano-sized cellulose fibers (nanofibrillated or bacterial cellulose) were reported to be used in composite aerogel approach, but nanocellulose reinforced aerogels were obtained via drying with sc CO_2

or via freeze drying techniques [24, 25, 30, 31]. The reason is that pores in-between cellulose fibrils are collapsing irreversibly during ambient pressure drying. Another disadvantage of using nanocellulose is that initially it is always dispersed in water and thus either freeze-drying, or water to alcohol exchange, is needed to be mixed with silica sol. Another polysaccharide, pectin, was recently used to obtain reinforced thermal superinsulating silica based aerogels, but here again drying was performed in sc conditions [32]. Our approach is established using ambient pressure drying of silica-based gel tailored for thermal superinsulation applications reinforced with highly uniform Tencel® cellulose fibers to obtain monolithic samples. To additionally validate our approach, fibers from wood pulp, flax, and recycled paper were also tested.

Materials and methods

Materials

Polyethoxydisiloxane (PEDS) solutions of prepolymerized oligomers of tetraethyl orthosilicate (TEOS) in ethanol with 20 wt% concentration of SiO_2 [33] were kindly provided by Enersens, France. Absolute ethanol was obtained from Fisher Scientific. 1,1,1,3,3,3-hexamethyldisilazane (HMDZ), 98% purity, was obtained from ACROS Organics. Aqueous ammonium hydroxide solution (NH_4OH) was purchased from Alfa Aesar. All chemicals were used as received. Water was distillated.

Tencel® fibers with diameter around 10 μm precut to 2 mm lengths were kindly provided by Lenzing AG, Austria. They are man-made cellulose fibers produced via dry wet-jet spinning from cellulose pulp dissolved in N-methyl-morpholine-N-oxide monohydrate (Lyocell process). Two types of non-bleached cellulose pulps with lignin content of 5 % and 12-15 wt% were kindly provided by Stora Enso, Finland. These pulp fibers contained 65-80 wt % of water when received, therefore were dried in the vacuum oven overnight at 60 ^oC

before use. Flax fibers were from Dehond, France, precut to 2 mm lengths. Recycled "wet strength paper" and "recycled magazine" fibers were kindly provided by Aerocycle GmbH, Germany. Optical microscope images of all fibers as utilized (after the expansion with the mill, see Methods section) are shown in Figure 1.

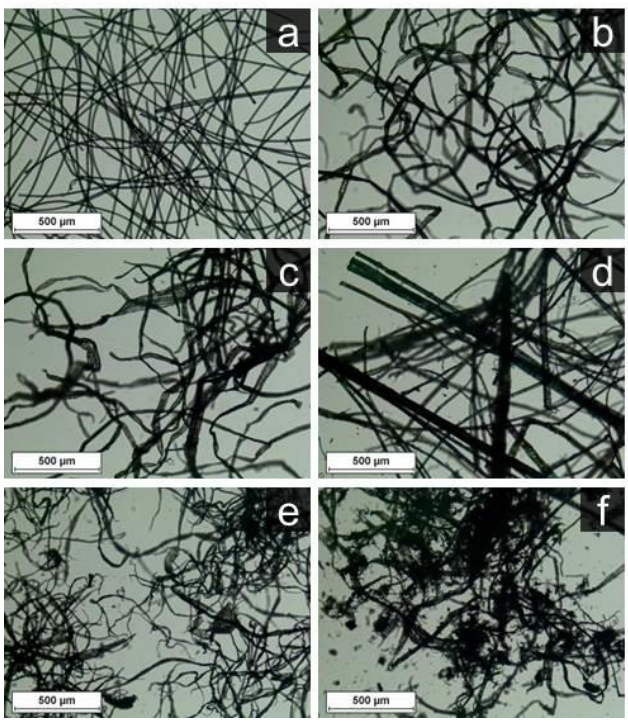

Fig. 1

Optical microscope images of mill expanded Tencel® (a), pulp with 5 wt% lignin (b), pulp with 12 wt% lignin (c), flax (d), recycled "wet strength paper" (e) and "recycled magazine" (f) fibers

Methods

Preparation of composite aerogels

The fibers were expanded by utilizing analytical sample mill "A 11 basic" from IKA, operating at maximum speed of 28000 rpm for 30 s, which resulted in fiber agglomerates' or bundles' separation and a significant volume increase. Figure 2 shows the same amount of Tencel® fibers (0.5 g) before and after the expansion with a mill. This treatment allowed

formation of a self-supporting three dimensional nonwoven fiber network. This expanded fiber network was impregnated with a PEDS-based sol. Most of the work presented in this article was performed with Tencel® which was considered as model fibers because of their known chemical composition (100% cellulose) and uniform diameter. Their concentration in silica sol was 1, 1.5, 2 and 3 wt% which resulted in 10, 15, 18 and 25 wt% in corresponding aerogel (i.e. final dried material). Fiber volume concentrations (vol %) in the aerogels were calculated for each case considering sample final volume and density of cellulose fibers 1.5 g/cm^3 [34]; the concentrations varied from about 0.7 to 2.1 vol%. Other fibers were used only to show the proof of concept and their concentration in dried aerogel was 25 wt% for flax and recycled paper and 35 wt% for the recycled magazine fibers.

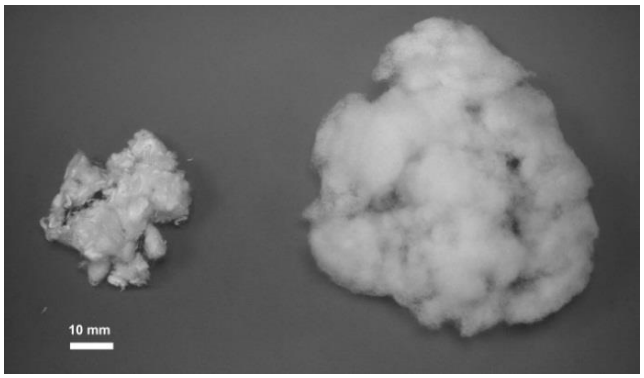

Fig. 2

0.5 g of the Tencel® fibers before (left) and after (right) they have been mechanically expanded with a mill

The schematic presentation of aerogel preparation is shown in Figure 3. Gels were synthesized in ambient conditions. The PEDS solution was diluted to 8 wt% concentration of SiO_2 with absolute ethanol. Sol-gel synthesis was initiated by adding solution of NH_4OH (1.6 M) at 7 % v/v of the sol under constant mechanical stirring at 300 rpm. After 30 seconds of such mixing, the sol was poured into cylindrical molds (48 mm diameter and 15 mm height) containing various quantities of expanded fibers prepared as described above. Gelation

occurred in approximately 15 minutes after addition of catalyst solution. Composite gels were covered with additional ethanol and aged in a lab oven (Memmert UN30) at 60 °C for 48 hours. After aging, the excess ethanol was removed and silylation was performed by covering the gels with HMDZ solution and keeping them for 72 h at ambient temperature. The silylated gels were then washed with ethanol and finally dried at 140 °C for 2 hours in the lab oven (Memmert ULE 400).

Reference aerogels were prepared in the same way but dried with supercritical (sc) CO_2. The samples were placed in a 1 L autoclave and covered with ethanol in order to avoid evaporative drying. Sealed autoclave was then pressurized with the CO_2 to 50 bar at 37 °C. The excess ethanol was drained while maintaining these conditions followed by pressurization to 80 bar and dynamic washing step with 5 kg of CO_2/h for 1 h. The system was then maintained in a static mode for 2 h in order to allow further diffusion of the sc CO_2 into the smallest pores of the sample. Another dynamic washing was then performed for 2 h at the same CO_2 feed rate and pressure, followed by slow depressurization at a rate of 4 bar/h while maintaining isothermal condition (37 °C). The autoclave was then cooled down to ambient temperature and the samples were collected for further characterization [35].

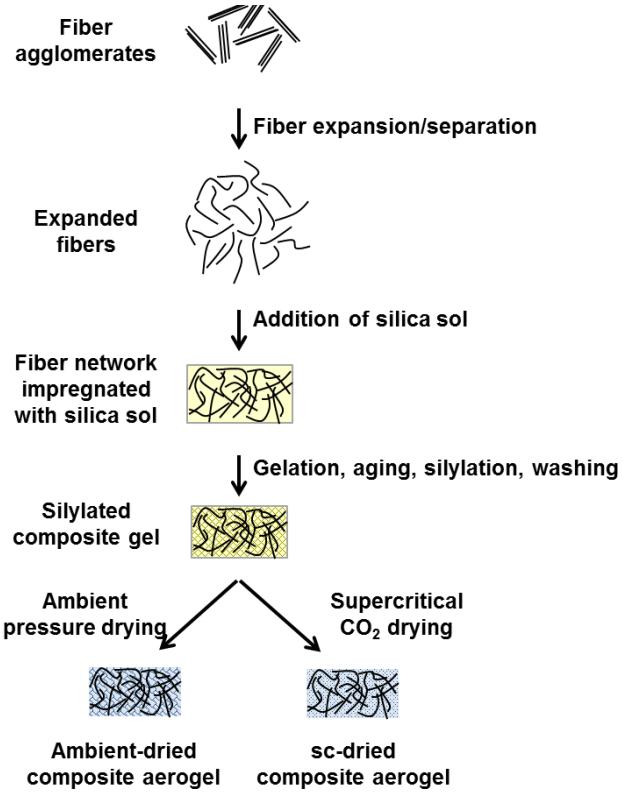

Fig. 3

Schematic presentation of the entire preparation process of composite aerogels

Characterization

Bulk density of composite aerogels was calculated from the final sample volume measured with a caliper and weight measured with an analytical balance (Mettler Toledo MS with 1 mg readability).

Scanning electron microscopy observations were performed using Zeiss Supra 40 FEG-SEM. Samples were sputter coated with a 7 nm platinum layer with a QUORUM Q150T before imaging. Philips XL30 environmental SEM was utilized for acquiring low magnification images of the samples without coating.

Specific surface area measurements based on N_2 adsorption BET theory were performed with the ASAP 2020 from Micromeritics. Samples were degassed in vacuum at 100 °C for 10 h before the measurement.

Water contact angle was measured using Drop Shape Analyser DSA100 (Krüss GmbH, Germany).

Thermal conductivity of the materials was evaluated using a Fox150 Thermal Conductivity Meter (Laser Comp) equipped with a custom micro-flow meter cell developed for small samples by CSTB (Grenoble, France) [36]. Thermal conductivity of the samples was calculated based on the heat flow measurement between two plates maintained at 25 ^{o}C and 15 ^{o}C.

Thermogravimetric analysis (TGA) was performed using Mettler Toledo TGA/SDTA851. The temperature was varied from 25°C to 800°C with a ramp of 10 °C.min^{-1} under nitrogen flow at 50 mL.min^{-1}.

Results and discussion

Cellulose fiber-silica alcogels and subsequent composite aerogels underwent a series of dimensional changes (mostly shrinkage) during the different preparation steps. The most significant variations were observed during the aging and the ambient-drying steps. Aging step is obviously the same for sc and ambient pressure dried aerogels. Cumulative volume decrease or shrinkage (%) was calculated according to eq. 1:

$$\boldsymbol{shrinkage}\ (\%) = (\mathbf{1} - \frac{\boldsymbol{v_i}}{\boldsymbol{v_0}})\mathbf{100}\% \qquad (1)$$

where v_0 and v_i are gel volumes at the initial and at ith processing step.

Shrinkage depends on the concentration of fibers in the composite. Higher fiber concentration leads to decrease of shrinkage occurring during the aging step. Likely the presence of the fibers inhibits movement of the mineral chains which occurs during aging because of the continuation of condensation reactions after sol-gel transition. For example, the shrinkage during aging of pure silica gel was 20 % ± 1 compared to 7 % ± 2 for the gel containing the largest concentration (25 wt%) of fibers.

Shrinkage during drying strongly depends on the mode of drying. Sc drying avoids creating capillary stresses and therefore is expected to preserve the solid network of the alcogel. The total shrinkage of the sc-dried gels therefore occurs essentially during sample aging. During the ambient evaporative drying, an additional shrinkage effect is observed. Figure 4 shows the slight difference between total shrinkage of sc-dried and ambient pressure dried aerogels as a function of fiber concentration.

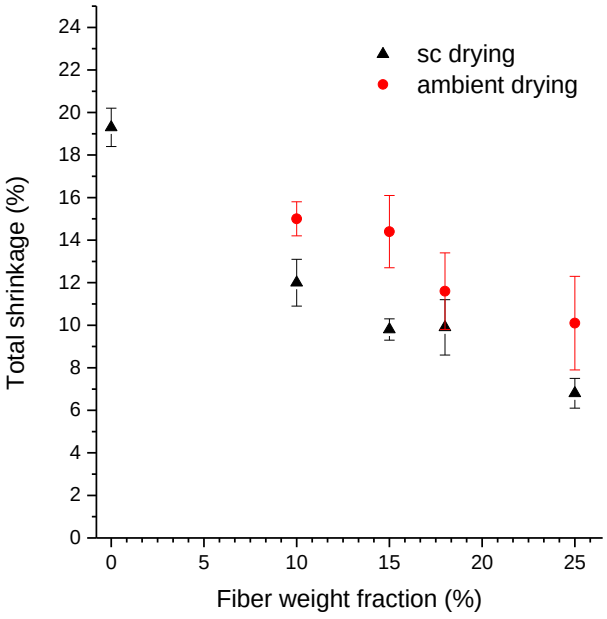

Fig. 4

Total sample shrinkage as a function of Tencel® fiber weight fraction for ambient-dried and sc-dried aerogels. (Monolithic ambient-dried aerogel without addition of fibers is not possible, therefore the shrinkage of this sample was not determined.)

During ambient pressure drying, hydrophobized gel is first contracting due to capillary pressure and then is undergoing a “spring-back” resulting in multiple fractures within the gel. In most of the cases, there is a loss of monolithic shape leading to divided beds constituted of granular objects. This effect is well known (and is the reason of the absence of cumulated

shrinkage value for ambient dried aerogels without fibers in this study). What is important here is that in the presence of short cellulose fibers the samples keep macroscopic monolithic shape despite internal silica fractionation during evaporative drying, in the same way as standard silica-based blankets synthesized with non-woven mats. Similar behavior was observed for all cellulose fiber-silica ambient dried composite aerogels evaluated in this study.

The illustration of pure silica and composite gels evolution in time during drying is shown in video 1 in the Electronic Supplementary Material. Images were captured using identical camera position and settings. The resulting video represents 2 hours of real time (300× real time speed). As expected, almost immediately after placing the gels in the oven, the evaporation of ethanol begins and cracks appear on the sample surface. As the drying progresses, pure silica gel breaks into pieces, but composite gel remains macroscopically intact. The contraction of the gel takes place during the initial 60 minutes of the drying and dimension changes are rather limited. This first step is followed by a slow recovery which commences at the end of the drying cycle. The global "spring-back" phenomenon is evident although it remains low, which is similar to standard silica-based blankets. The final shrinkage of our composite aerogels is less than 15 vol% (Figure 4). The shrinkage recorded is not as drastic as reported in the literature for some ambient dried monolithic aerogels prepared with polymethylsilsesquioxane precursors (PMSQ) [19]. Such PMSQ-based ambient dried aerogels exhibit between 40% and 60 % linear shrinkage before linear recovery of 25%. It is worth noting that these aerogels have a different silica network structure as compared with ours, and therefore different pore structure and ultimately different properties in the wet stage. However, PMSQ aerogels are also thermally superinsulating materials which makes this comparison consistent.

The bulk density of sc and ambient dried aerogels varied from 0.1 to 0.13 g/cm^3 for fiber concentrations from 0 to 25 wt%, respectively (Figure 5). Small difference of densities between the two families of aerogels for the lower fiber fraction was evident, likely due to a higher shrinkage during the ambient drying. An increase in density was observed as the fiber fraction was increased for all samples. This clearly shows that addition of matter (i.e. fibers) in the gels is governing the evolution of bulk density instead of sample shrinkage.

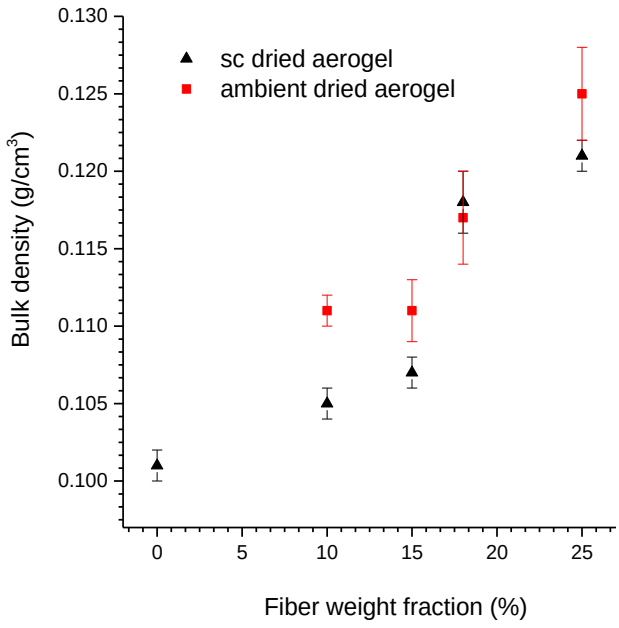

Fig. 5

Bulk density of composite aerogels as a function of Tencel® fibers concentration and drying mode

Specific surface areas as measured by BET method are shown in Figure 6. The values are very similar for both types of composite aerogels, considering the experimental errors. Without fibers, specific surface area is the highest, around 730 m^2/g, which is in quantitative agreement with what has been previously reported for this type of silica aerogels [32]. Fiber addition affects the specific surface area regardless of the drying mode. As expected, specific

area is decreasing with the increase of fibers concentration in the composites. The theoretical specific surface area (dashed line in Figure 6) was calculated according to a simple "mixing rule" based on the specific surface area of pure silica aerogels. We assumed that the fiber contribution to this parameter is zero since the specific surface area of the cellulosic fibers is negligibly low compared to the one of the silica matrix. Small experimental deviation from linearity demonstrates that the presence of fibers does not significantly affect specific surface area of the silica matrix itself (Figure 6). It is also worth noting that even with the highest amount of fibers present in composite aerogels, i.e. 25wt%, BET specific surface area remains high, higher than 570 m^2/g.

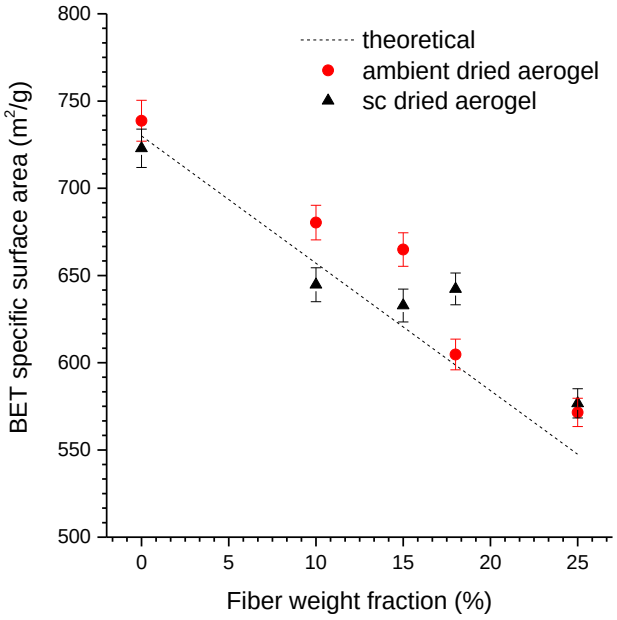

Fig. 6

BET specific surface areas of the aerogel composites. Dashed line corresponds to the theoretical specific surface area (see details in the text)

High magnification SEM shows silica phase alone for sc and for ambient dried composite aerogels (Figure 7a and b, respectively). Highly porous structure of the silica is

preserved during the subcritical drying and remains in the mesopore range, as specific surface data shows.

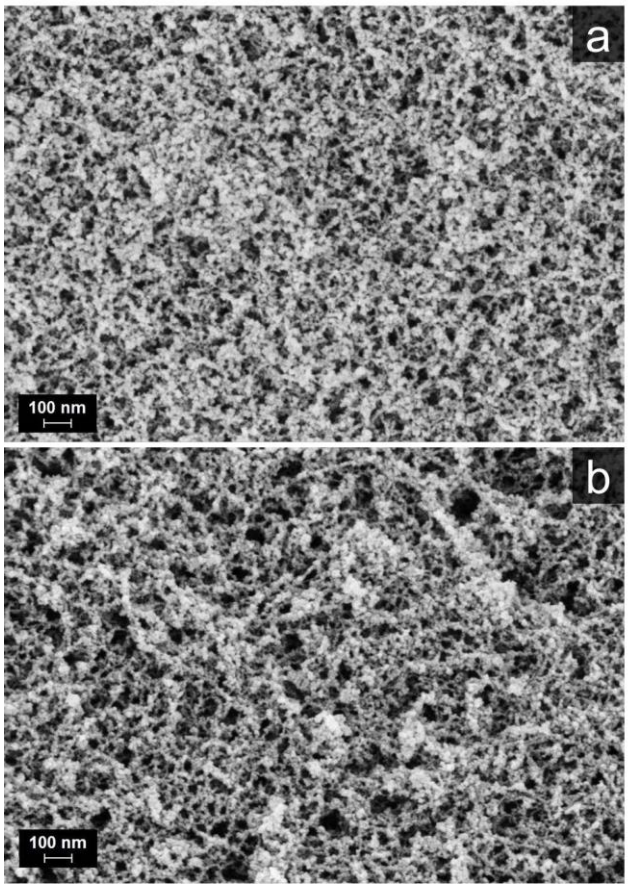

Fig. 7

SEM images of silica phase in sc dried (a) and ambient dried (b) aerogels

For using aerogels for thermal insulation, hydrophilic/hydrophobic balance is very important. Table 1 shows water contact angle for all formulations; it is unaffected by the presence of fibers or by the gel drying method. All samples remain highly water repellant regardless of the formulation. This is specifically due to the silylation with HMDZ [37]. Figure 8 illustrates the typical hydrophobic behavior with the water droplets beading up on the sample surface. The volume fraction of fibers is very low, below 2.5 vol%, and fibers are distributed in highly hydrophobic silica, as shows SEM image in Figure 9. Cellulose fibers

form a network in between silica “holding” it together. Figure 9b shows SEM image highlighting that there is no chemical bonding between the silica matrix and cellulosic fibers.

Table 1**.** Water contact angles of ambient dried and sc dried aerogels. Ambient dried aerogels without fibers are not monolithic, therefore the water contact angle of these samples was not measured.

Fiber weight fraction (%)	Fiber volume fraction (%)	Water contact angle (^{o})
Ambient dried aerogels		
0	0	NA
10	0.71	133 ± 8
15	1.07	138 ± 3
18	1.42	137 ± 9
25	2.11	139 ± 8
Supercritical CO_2 dried aerogels		
0	0	142 ± 4
10	0.70	136 ± 2
15	1.03	138 ± 1
18	1.36	142 ± 5
25	2.02	140 ± 2

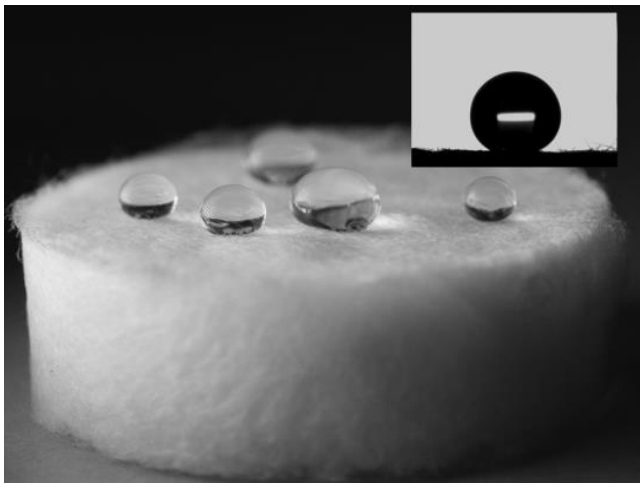

Fig. 8

Water droplets (4 μl droplet in the inset photo) on the surface of the Tencel® fiber – silica ambient pressure dried aerogel (18 wt % fiber content) showing highly hydrophobic surface with the water contact angle around 138 °

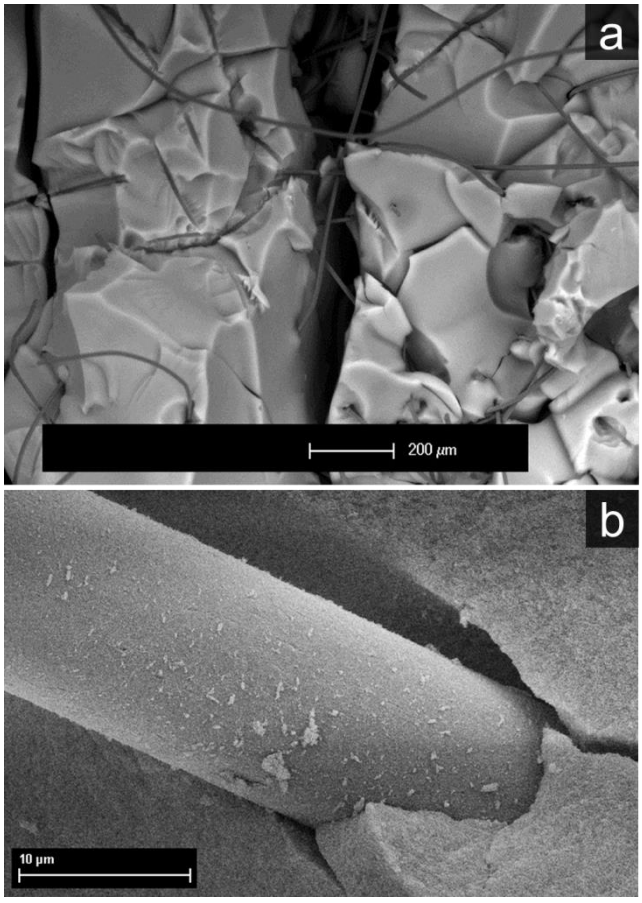

Fig. 9

SEM image of ambient dried aerogel with Tencel® fibers (18 wt %, 1.42 vol%) at two magnifications

Thermal conductivity of the sc and ambient-dried aerogels is shown in Figure 10. In both cases it slightly increased with an increase of fiber concentration (no more than by 0.004 W/m.K compared to pure silica sc dried aerogel), still remaining in superinsulation region at the highest fiber concentration. This increase is unsurprising because the thermal conductivity of the cellulose fibers is much higher than that of the silica aerogel, and bulk density of the composites increases with the increase of fiber fraction. For example, the thermal conductivity of cellulose nanocrystals is the highest, from 0.72 to 5.7 W/m.K [38], of their organized nanostructured films it is 0.22-0.53 W/m.K [38], of different wood it is around 0.2-0.4 W/m.K [39] and of natural fiber cell wall 0.54 W/m.K [40]. The thermal conductivity values of the ambient-dried aerogels were on average only about 7 % higher than those for their sc dried counterparts. This may be due to some macroscopic cracks formed during ambient drying which are likely too large to take advantage of the Knudsen effect.

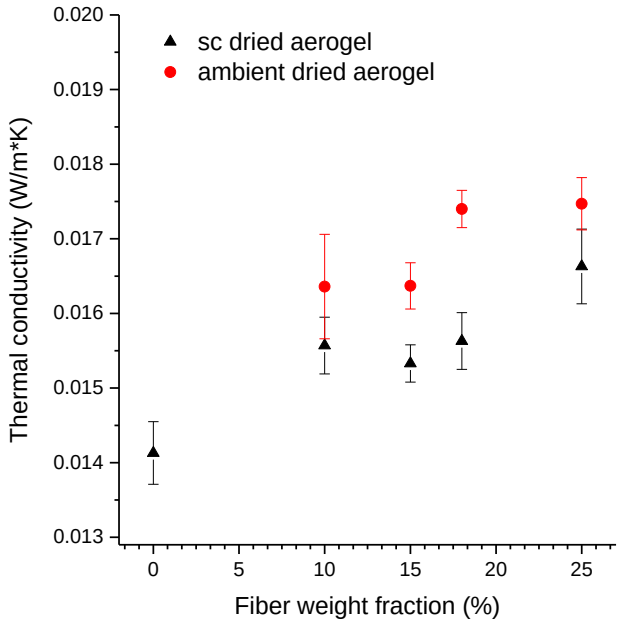

Fig. 10

Thermal conductivity of Tencel® fibers–silica composite aerogels prepared via ambient pressure and sc drying. (Because ambient dried pure silica aerogel is fractured during drying, thermal conductivity cannot be measured at zero fiber concentration.)

A variety of other cellulosic fibers (see Materials section) were used to prepare ambient pressure dried composite aerogels and demonstrate the feasibility of our original approach. All samples were prepared in the same way as described for Tencel® fibers. The main property of use, i.e. thermal conductivity, was measured. In all cases it was possible to prepare monolithic samples which demonstrates the proof of concept established with model fibers such as Tencel®.

Figure 11 shows that composite aerogel with high lignin containing pulp has the same thermal conductivity as Tencel®-based counterpart with the same fiber fraction. This is a very interesting result which shows that high purity cellulose is not needed for making monolithic and thermal superinsulating ambient-dried aerogels. Interestingly, unbleached pulp with the lignin content around 5 wt% showed the highest value of thermal conductivity among this set

of samples, 0.022 W/m.K. This is most likely due to the fact that being used as received, this pulp kept the traces of alkaline treatment used for the removal of lignin. The pH of pulp-water dispersion was around 9. It is well known that silica dissolution as well as sol-gel reaction (both hydrolysis and condensation mechanisms) and therefore the morphology of silica aerogel itself are very sensitive to pH [41]. The possible modification of silica sol pH induced by fibers could thus affect morphology of the aerogel towards a more colloidal internal structure and, and as a potential consequence, affecting thermal conductivity.

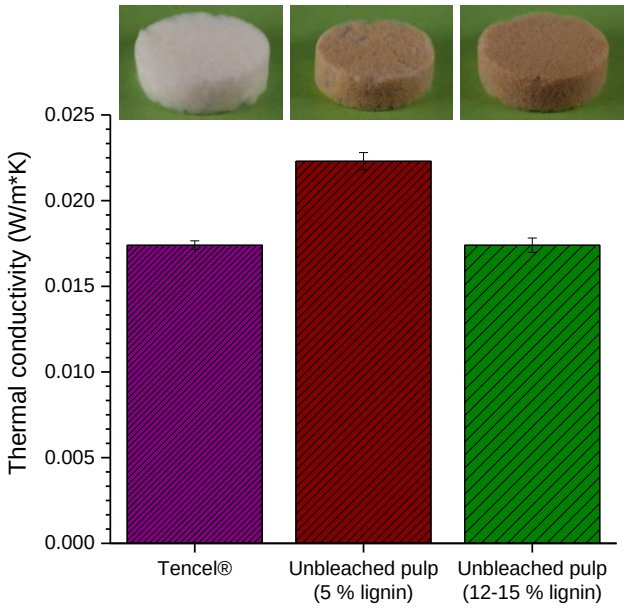

Fig. 11

Thermal conductivity of ambient-dried aerogels prepared with different cellulose pulps, Tencel® fiber-silica ambient dried aerogel is also shown for comparison. All samples have fiber concentration of 18 wt%

Slightly higher values of conductivity were recorded for composite aerogels with flax and recycled paper (Figure 12), around 0.020 – 0.021 W/m.K in room conditions. Flax, being expanded, still contained undissociated bundles which were not completely disrupted during

the milling process (see Figure 1). The presence of "thick" fibers could potentially increase the conductivity of the solid phase. The same reason can be given for aerogels with fibers from recycled paper: they are of very irregular and sometimes large diameter (Figure 1). Additionally, it is worth noting that due to the reduced fiber length and ultimately aspect ratio of these fibers, higher fiber concentration had to be used in order to achieve fiber percolation throughout the sample and obtain monolithic samples. However, they all remained in the thermal super-insulation region, i.e. below thermal conductivity of free air in standard conditions (0.025 W/m.K).

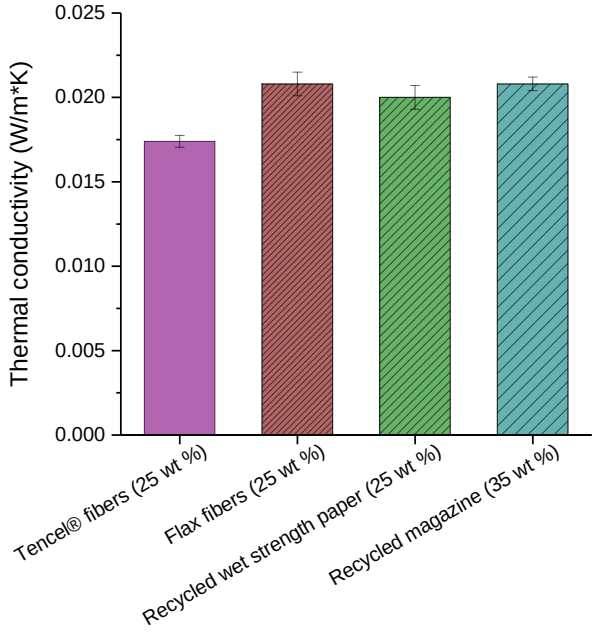

Fig. 12

Thermal conductivity of ambient-dried aerogels prepared using raw and recycled cellulose based fibers. Tencel® fiber-silica composite is shown for comparison.

Low thermal conductivities observed for the ambient-dried aerogels regardless of the type of cellulosic fiber used indicate that in most of the cases shown the mesoporous structure of the silica has been preserved as well as the nanostructure of its solid backbone. A

commercial fiber glass insulation is typically accepted to have thermal conductivity in the range of 0.04 W/m.K, and the commercial blanket-type aerogel based insulating composites are usually advertised to have thermal conductivities between 0.014 – 0.020 W/m.K. The aerogels prepared using our approach, with short cellulose fibers, compare very favorably with the best advanced products actually available. Small variations of thermal conductivities between the different cellulosic fibers indicate that fiber network structure and and morphology and properties of the fibers themselves may influence the conductivity values. It is therefore reasonable to expect that even lower conductivities of aerogels prepared using ambient pressure drying are possible by further fiber network optimization.

The thermal behavior of silica-based composite aerogels under elevated temperatures was also investigated by TGA. The analysis was performed on non-hydrophobized and HMDZ-treated sc dried pure silica aerogels, on Tencel® fibers alone and on ambient-dried composite aerogels (Figure S1 of Supplementary Information). The weight loss of non-hydrophobized materials, silica aerogel and Tencel®, starts around 50 – 60 °C due to dehydration. For non-hydrophobised silica aerogel the total weight loss is around 10 %.The main weight losses of Tencel® occurs in two steps, around 350 °C and 500 °C. The pyrolysis of cellulose is a complex process: it starts with cellulose depolymerisation and formation of levoglucosan which is then decomposed into various anhydrosugars, which in turn can react and form unstable intermediates (furanes, volatile substances) and char [42, 43]. At 500 °C, thermal degradation is finished and 90 % of the initial mass is lost. HMDZ-treated silica aerogel starts to lose weight around 310 °C due to the oxidation of the methyl groups (grafted during silylation step) cleaved from the silica network [44]. Finally, the mass of composite aerogel decreases first at the same temperature as that of hydrophobised silica aerogel and further decreases due to cellulose degradation. At around 500 °C thermal degradation is over and the composite lost around 40 % of its initial mass.

Conclusions

Tencel® fibers were used to prepare monolithic, low density and highly hydrophobic silica-based ambient dried aerogels with thermal conductivity around 0.016 – 0.017 W/m.K in room conditions by simple subcritical evaporative drying. Cellulose fibers served to "support" mesoporous and nanostructured silica network from defragmentation during ambient drying. Cellulose fibers accommodate the contraction and re-expansion of the silica phase caused by the evaporation of the solvent at ambient pressure and moderate temperature. The internal morphology of the silica matrix is preserved, e.g. high specific surface area. It was demonstrated that this simple processing method is applicable for a wide variety of cellulosic fibers ranging from man-made cellulose (Tencel®) to natural fibers as well as recycled cellulosic fibers.

Acknowledgements

The French Agency for Environment and Energy Management (ADEME) is acknowledged for financial support. The authors are also very grateful to Lenzing, Stora Enso and Aerocycle for providing fibers, pulps and recycled fiber, respectively, as well as Enersens for providing PEDS solutions. Authors thank Pierre Ilbizian (MINES ParisTech – PERSEE) for sc CO_2 drying, Julien Jaxel (MINES ParisTech – CEMEF) for pulp fiber preparation and TGA analysis, university of Nice for allowing performing TGA experiments, and Suzanne Jacomet (MINES ParisTech – CEMEF) for SEM.

Electronic supplementary material: The online version of this article (doi:xxxxxxxxx) contains supplementary material, which is available to authorized users.

References

[1] Hrubesh LW (1998) Aerogel applications, J Non-Cryst Solids 225:335-342

[2] Fricke J, Lu X, Wang P, Büttner D, Heinemann U (1992) Optimization of monolithic silica aerogel insulants, Int J Heat Mass Tran 35(9):2305-2309

[3] Pierre AC, Rigacci A (2011) SiO_2 aerogels. In: Aegerter MA, Leventis N, Koebel MM (eds) Aerogels Handbook. Springer, New York

[4] Baetens R, Jelle BP, Gustavsen A (2001) Aerogel insulation for building applications: a state-of-the-art review, Energ Buildings 43:761-769

[5] Koebel M, Rigacci A, Achard P (2012) Aerogel-based thermal superinsulation: an overview, J Sol-Gel Sci Technol 63:315-339

[6] Jelle BP (2011) Traditional, state-of-the-art and future thermal building insulation materials and solutions – properties, requirements and possibilities, Energ Buildings 43:2549-2563

[7] Cuce E, Cuce PM, Wood CJ, Riffat SB (2014) Toward aerogel based thermal superinsulation in buildings: a comprehensive review, Renew Sustain Energy Rev 34:273-99

[8] Zeng SQ, Hunt AJ, Cao W, Greif R (1994) Pore size distribution and apparent gas thermal conductivity of silica aerogel, J Heat Trans-T ASME 116:756-759

[9] Notario B, Pinto J, Solorzano E, de Saja JA, Dumon M, Rodriguez-Perez MA (2015) Experimental validation of the Knudsen effect in nanocellular polymeric foams, Polymer 56:57-67

[10] Caps R, Fricke J (1985) Determination of the radiative heat transfer in transparent silica aerogel, Int J Sol Energ 3(1):13-18

[11] Bisson A, Rigacci A, Lecomte D, Rodier E, Achard P (2003) Drying of silica gels to obtain aerogels: phenomenology and basic techniques, Dry Technol 21(4):593-628

[12] Tewari PH, Hunt AJ, Lofftus KD (1985) Ambient-temperature supercritical drying of transparent silica aerogels, Matter Lett 3(9-10):363-367

[13] Smith DM, Deshpande R, Brinke CJ (1992) Preparation of low-density aerogels at ambient pressure, MRS Symp Proc 271:567-572

[14] Schwertfeger F, Frank D, Schmidt M (1998) Hydrophobic waterglass based aerogels without solvent exchange or supercritical drying, J Non-Cryst Solids 225:24-29

[15] Wang LJ, Zhao SY, Yang M (2009) Structural characteristics and thermal conductivity of ambient pressure dried silica aerogels with one-step solvent exchange/surface modification, J Mater Chem Phys 113:485-490

[16] Mahadik DB, Rao AV, Kumar R, Ingale SV, Wagh PB, Gupta SC (2012) Reduction of processing time by mechanical shaking of ambient pressure dried TEOS based silica aerogel granules, J Porous Mater 19:87-94

[17] Fesmire JE (2006) Aerogel insulation systems for space launch applications, Cryogenics 46:111-117

[18] Bardy ER, Mollendorf JC, Pendergast DR (2007) Thermal conductivity and compressive strain of aerogel insulation blankets under applied hydrostatic pressure, J Heat Trans-T ASME 129:232-235

[19] Hayase G, Kanamori K, Maeno A, Kaji H, Nakanishi K (2016) Dynamic spring-back behavior in evaporative drying of polymethylsilsesquioxane monolithic gels for low-density transparent thermal superinsulators, J Non-Cryst Solids 434:115-119

[20] Einarsrud MA (1998) Light gels by conventional drying, J Non-Cryst Solids 225:1-7

[21] Maleki H, Duraes L, Portugal A (2014) An overview on silica aerogels synthesis and different mechanical reinforcing strategies, J Non-Cryst Solids 385:55-74

[22] Li L, Yalcin B, Nguyen BN, Meador MAB, Cakmak M (2009) Flexible nanofiber-reinforced aerogel (xerogel) synthesis, manufacture, and characterization, ACS Appl Mater Interfaces 1(11):2491-2501

[23] Li X, Wang Q, Li H, Ji H, Sun X, He J (2013) Effect of sepiolite fiber on the structure and properties of the sepiolite/silica aerogel composite, J Sol-Gel Sci Technol 67:646-653

[24] Hayase G, Kanamori K, Abe K, Yano H, Maeno A, Kaji H, Nakanishi K (2013) Polymethylsilsesquioxane-cellulose nanofiber biocomposite aerogels with high thermal insulation, bendability, and superhydrophobicity, ACS Appl Mater Interfaces 6:9466-9471

[25] Zhao S, Zhang Z, Sèbe G, Wu R, Virtudazo RVR, Tingaut P, Koebel M (2015) Multiscale assembly of superinsulating silica aerogels within silylated nanocellulosic scaffolds: improved mechanical properties promoted by nanoscale chemical compatibilization, Adv Funct Mater 25(15):2326-2334

[26] Fu J, Wang S, He C, Lu Z, Huang J, Chen Z (2016) Facilitated fabrication of high strength silica aerogels using cellulose nanofibrils as scaffold, Carbohyd Polym 147:89-96

[27] John MJ, Thomas S, (2008) Biofibres and biocomposites, Carbohyd Polym 71:343-364

[28] Jawaid M, Abdul Khalil HPS (2011) Cellulosic/synthetic fibre reinforced polymer hybrid composites: A review, Carbohyd Polym 86:1-18

[29] Joshi SV, Drzal LT, Mohanty AK, Arora S (2004) Are natural fiber composites environmentally superior to glass fiber reinforced composites? Compos Part A 35:371-376

[30] Wong JCW, Kaymak H, Tingaut P, Brunner S, Koebel MM (2015) Mechanical and thermal properties of nanofibrillated cellulose reinforced silica aerogel composites, Micropor Mesopor Mat 217:150-158

[31] Sai H, Xing L, Xiang J, Cui L, Jiao J, Zhao C, Li Z, Li F (2013) Flexible aerogels based on an interpenetrating network of bacterial cellulose and silica by non-supercritical drying process, J Mater Chem A 1:7963-7970

[32] Zhao S, Malfait WJ, Demilecamps A, Zhang Y, Brunner S, Huber L, Tingaut P, Rigacci A, Budtova T, Koebel MM (2015) Strong, thermally superinsulating biopolymer-silica aerogel hybrids by cogelation of silicic acid with pectin, Angew Chem Int Ed 54:14282-14286

[33] Demilecamps A, Beauger C, Hildenbrand C, Rigacci A, Budtova T (2015) Cellulose – silica aerogels, Carbohyd Polym 122:293-300

[34] Netravali AN, Chabba S (2003) Composites get greener, Mater today 6(4):22-29

[35] Masmoudi Y, Rigacci A, Ilbizian P, Cauneau F, Achard P (2006) Diffusion during the supercritical drying of silica gels, Dry technol 24(9):1121-1125

[36] Rudaz C, Courson R, Bonnet L, Calas-Etienne S, Sallée H, Budtova T (2014) Aeropectin: fully biomass-based mechanically strong and thermal superinsulating aerogel, Biomacromolecules 15(6):2188-2195

[37] Yokogawa H, Yokoyama M (1995) Hydrophobic silica aerogels, J Non-Cryst Solids 186:23-29

[38] Diaz JA, Ye Z, Wu X, Moore AL, Moon RJ, Martini A, Boday DJ, Youngblood JP (2014) Thermal conductivity in nanostructured films: from single cellulose nanocrystals to bulk films , Biomacromolecules 15:4096-4101

[39] Gupta M, Yang J, Roy C (2003) Specific heat and thermal conductivity of softwood bark and softwood char particles, Fuel 82:919–927

[40] Sekino N (2016) Density dependence in the thermal conductivity of cellulose fiber mats and wood shavings mats: investigation of the apparent thermal conductivity of coarse pores, J Wood Sci 62:20-26

[41] Brinker CJ, Scherer GW (1990) Sol-gel science. Academic Press

[42] S. Li, J. Lyons-Hart, J. Banyasz, K. Shafer (2001) Real-time evolved gas analysis by FTIR method: an experimental study of cellulose pyrolysis, Fuel 80:1809-1817

[43] Y.-C. Lin, J. Cho, G. A. Tompsett, P. R. Westmoreland, G. W. Huber (2009) Kinetics and Mechanism of Cellulose Pyrolysis, J. Phys. Chem. C, 113:20097–20107

[44] A. P. Rao, A. V. Rao, G. M. Pajonk, P. M. Shewale (2007) Effect of solvent exchanging process on the preparation of the hydrophobic silica aerogels by ambient pressure drying method using sodium silicate precursor, J Mater Sci 42:8418–8425

Figure captions

Fig. 1

Optical microscope images of mill expanded Tencel® (a), pulp with 5 wt% lignin (b), pulp with 12 wt% lignin (c), flax (d), recycled "wet strength paper" (e) and "recycled magazine" (f) fibers

Fig. 2

0.5 g of the Tencel® fibers before (left) and after (right) they have been mechanically expanded with a mill

Fig. 3

Schematic presentation of the entire preparation process of composite aerogels

Fig. 4

Total sample shrinkage as a function of Tencel® fiber weight fraction for ambient-dried and sc-dried aerogels. (Monolithic ambient-dried aerogel without addition of fibers is not possible, therefore the shrinkage of this sample was not determined.)

Fig. 5

Bulk density of composite aerogels as a function of Tencel® fibers concentration and drying mode

Fig. 6

BET specific surface areas of the aerogel composites. Dashed line corresponds to the theoretical specific surface area (see details in the text)

Fig. 7

SEM images of silica phase in sc dried (a) and ambient dried (b) aerogels

Fig. 8

Water droplets (4μl droplet in the inset photo) on the surface of the Tencel® fiber – silica ambient pressure dried aerogel (18 wt % fiber content) showing highly hydrophobic surface with the water contact angle around 138 °

Fig. 9

SEM image of ambient dried aerogel with Tencel® fibers (18 wt %, 1.42 vol%) at two magnifications.

Fig. 10

Thermal conductivity of Tencel® fibers–silica composite aerogels prepared via ambient pressure and sc drying. (Because ambient dried pure silica aerogel is fractured during drying, thermal conductivity cannot be measured at zero fiber concentration.)

Fig. 11

Thermal conductivity of ambient-dried aerogels prepared with different cellulose pulps, Tencel® fiber-silica ambient dried aerogel is also shown for comparison. All samples have fiber concentration of 18 wt%

Fig. 12

Thermal conductivity of ambient-dried aerogels prepared using raw and recycled cellulose based fibers. Tencel® fiber-silica composite is shown for comparison

SUPPLEMENTARY INFORMATION

Ambient-dried thermal superinsulating monolithic silica-based aerogels with short cellulosic fibers

Gediminas Markevicius[1, 2], Rachid Ladj[1, 2], Philipp Niemeyer[1, 2]

Tatiana Budtova[2]*, Arnaud Rigacci[1]*

[1] MINES ParisTech, PSL Research University, PERSEE - Centre for processes, renewable energy and energy systems, CS 10207 rue Claude Daunesse, 06904 Sophia Antipolis Cedex, France

[2] MINES ParisTech, PSL Research University, CEMEF - Centre for Materials Forming, CNRS UMR 7635, rue Claude Daunesse, CS 10207, 06904 Sophia Antipolis Cedex, France

Figure S1.

TGA of sc CO_2 dried pure silica aerogel hydrophobized with HMDZ (1) and not (2), ambient pressure dried silica-based composite aerogel with 15 wt% of 8 mm Tencel® (3) and Tencel® fibers alone (4).